https://dx.doi.org/10.4314/ijs.v24i2.14

Ife Journal of Science vol. 24, no. 2 (2022)

PETROGENETIC CHARACTERISATION AND PALEO-CLIMATIC STUDY OF SOME CLAY OCCURRENCES OVER PRE-CAMBRIAN BASEMENT COMPLEX IN SOUTHWESTERN NIGERIA

Afolabi, O.O.[1] **and Afolabi, O.A.**[2,*]
[1]Department of Geology, Afe Babalola University, Ado-Ekiti, Nigeria.
[2]Department of Earth Sciences, Ladoke Akintola University of Technology (LAUTECH), Ogbomoso, Nigeria.
*** Corresponding Author's Email:** oaafolabi@lautech.edu.ng

(Received: 1st February, 2022; Accepted: 5th September, 2022)

ABSTRACT

Bulk clay chemistry from specific areas underlain by Precambrian rocks composed of migmatitic gneiss, schist, charnockite and granite in Ekiti, Southwest Nigeria, was studied for their elemental compositions in order to assess petrogenesis and paleoclimatic conditions. Eleven representative clay samples were collected from various clay occurrences based on the underlying geology. The clay samples were prepared and analysed using X-ray Fluorescence (XRF). The XRF data on eleven representative samples revealed major oxides (wt. %) and trace element (ppm) concentrations. SiO_2 values ranged from 41.29 to 58.03 while Al_2O_3 and Fe_2O_3 values ranged from 15.86 to 36.61 and 0.27 to 13.05 respectively. Standard deviation (S.D) values of SiO_2 (4.2), Al_2O_3 (6.7) and Fe_2O_3 (4.8) suggested variable mobility. Average value of K_2O (1.46) is observed to be lower than average Upper Continental Crustal UCC) value (3.39) and may be due to intense weathering. Average concentration values of Zr (634.53 ppm), Nb (76.45 ppm) and Ta (29.19 ppm) were higher than their corresponding average values reported for UCC. Average values of Chemical Index of Alteration (CIA) and Plagioclase Index of Alteration (PIA) (CIA, 70 and PIA, 73) showed moderate to high intensity weathering. Ba/Sr vs Y/Sr values discriminated the clay occurrences over schist from migmatitic gneiss and granitoids. Kaolinisation in moderate to high weathering intensities under a dominant oxic condition was inferred from the plots of A-CN-K and Ni/Co vs Mafic Index of Alteration (MIA).

Keywords: Clays; Weathering; Precambrian rocks; Kaolinisation; Oxic, Paleo-climatic conditions.

INTRODUCTION

Weathering of feldspar/mica rich rocks is a dominant process in the formation of clays. Clays thus formed have their bulk chemistries derived through selective removal of elements such as Ca, Na, P, K, Sr, Ba, Rb, Mg and Si (Millot, 1970; Middleburg *et al.*, 1988; Galan *et al.*, 1998; Murray, 2007; Velde and Meunier, 2008). McLennan *et al.* (1993) and Galan *et al.* (1998) showed that the properties of clays with the same origin are similar but different from clays of different origins. The mode of formation of clays and their types help in defining their uses. Clays have found very important uses in human lives e.g. absorbents of grease and oil, drilling mud, sealants in landfills and harmful compounds waste site, binders in pharmaceutical, cosmetics and paint industries. Recently, clays have become good sources of rare earth elements (REEs) and are termed as ion-adsorbed clays (Yaraghi, *et al.*, 2019; Borst, *et al.*, 2020).

The use of clays is dependent on its mineralogical and chemical compositions. This in turn is based on the nature of the parent rocks and method of alteration. Alteration of feldspar-rich rocks yields different clay minerals. For example, alkali-granite typically yields kandites from the decomposition of orthoclase; shale (pelites), rich in feldspars and micas, would yield illites; and basic rocks, rich in plagioclase, would yield montmorillonite or smectites. The formation of clays and clay minerals has been attributed to weathering of rock materials under: i. rock-atmosphere interface, ii. sediment-water interface (deep sea or lake bottom), iii. the interaction of aqueous solutions and rock. The alteration of clay does not only influence the clay mineral types that can be formed but affects, also, the geochemical characters of clays. These geochemical characters depend on rock types. For instance, metal accumulations such as Au and U are linked with clay formation by hydrothermal alteration of rocks of magmatic origin (Galan and Farrell, 2013); Zn and Cu in clay minerals derived from rocks of sedimentary origin (Brigatti *et al.*, 2013).

In order to assess the degree of alteration of parent rocks, several weathering indices have been developed from molecular proportions of major oxides. Chemical Index of Alteration (CIA), Plagioclase Index of Alteration (PIA), Mafic Index of Alteration (MIA) and Index of Lateritisation (IOL) are some of the indices used in this study for evaluating intensity of weathering. Elemental removal/mobility associated with weathering can occur at early, intermediate and advanced stages of weathering. Calcium, Mg, Na and K are removed selectively with leaching of Fe during intense weathering. Clay minerals are built on the Si-tetrahedral (T) and Al-octahedral (O) sheets/layers. The sheets of the clay minerals, like other phyllosilicates, form either as T:O (1:1) or T:O:T (2:1) sheets as weathering progresses from intermediate to extreme weathering (Bergaya and Lagaly, 2013). The arrangement of these layers allows for the coordination of oxygen (O^{--}) and hydroxyl (OH^{-}) ends of the tetrahedral and octahedral layers, respectively, with other metals.

The chemistry and structure of Si-tetrahedral with Al-octahedral combinations give clays their properties. These properties (adsorption and absorption, plasticity, shrinkage under fire and air drying, fineness of grain, colour after firing, hardness, cohesion and capacity of the surface to take decoration) have been the main considerations for clay beneficiations.

Clay occurrences are found widely distributed across Nigeria (Adeleye, 1971; Adeleye and Dessauvagie, 1972; Akhirevbulu *et al*., 2010; Adelabu, 2012; Alege *et al.,* 2014; Aramide *et al.,* 2014; Dansarai, *et al.,* 2020). The present work evaluates the geochemical character of some clay occurrences in southwestern Nigeria with the aim of identifying possible parent rock and paleo-climatic conditions.

GEOLOGY OF THE STUDY AREA

Ekiti, a state in southwestern Nigeria, is underlain predominantly by Precambrian lithologies with several occurrences of clay. Archean Migmatitic Gneiss Complex of southwestern Nigeria stretches over more than half the total land cover of the study area (Figure 1). These parent bodies may be possible progenitors for the vast clay occurrences in the area. Clay occurrences were observed in Isan, Ijero, Ara and Ikere parts of Ekiti State.

In the area, Mid - Neo Proterozoic supracrustal and Pan African granitoids occur in close contact with the Archean migmatitic gneiss. The migmatitic gneiss in the area is made up of grey gneiss covering about 60 – 70% of the total land area of Ekiti. Felsic and mafic bands defining the foliation are composed of quartz – plagioclase and alkali feldspar - hornblende and biotite (Ayodele and Akinyemi, 2014). Other components are granitic unit and mafic – ultramafic units. The granitic units or granite gneiss, exposed as hilly topographic highs, were observed around Ado-Ekiti, southwest of the area. The granitic bodies at Ado-Ekiti, closely associated with charnockite, are porphyritic and biotite-hornblende rich. The mafic – ultramafic units are amphibolitic in composition. They occur as xenoliths and boudinaged fragments within host rocks. The amphibolitic unit is dominantly composed of hornblende, plagioclase, biotite, quartz while sphene and opaque minerals were reported as accessory minerals. Quartzites occurrences are localised at the northwest of the area studied (Figure 1) and occur as mega isoclinal fold whose parallel limbs trend N-S direction. The quartzite occurs as both massive and schistose in outcrop. The schistose quartzite occurs as layered quartz blocks separated by thin sheets of muscovite.

Pelitic units described as undifferentiated metasediment schist (Figure 1) occur closely with quartzitic units and are restricted to the northwest of the study area. This pelitic unit contains quartz, plagioclase, biotite, sillimanite, cordierite and garnet (Ale *et al*., 2014). The schistose units are observed to be intruded by pegmatitic bodies which are composed of quartz, feldspar, biotite and tourmaline (Obasi and Madukwe, 2016).

Olarewaju (1987) described three textural varieties of granites: i. the fine- to medium-grained biotite granite, ii. the medium- to coarse-grained non-porphyritic biotite hornblende granite and iii. the porphyritic biotite hornblende granite. The occurrence of granite in the area covers more area than the charnockites of igneous origin. The charnockitic bodies in the study area were distinguished based on texture as i) the coarse-grained variety, ii) the massive/non-foliated fine-grained variety and iii) the foliated fine-grained variety. Charnockite bodies outcropped as elongated intrusives, structurally, partitioning the medium grained granite/porphyritic granite bodies, or as discrete bodies within the migmatitic gneiss complex. They have been described to occur at the core of granitic or as elongated marginal units or dykes (Olarewaju, 1981; Rahaman, 1988). The mineralogy of charnockite in the study is typical of granite (quartz + alkali feldspar + plagioclase ± hornblende ± zircon ± allanite) with the addition of orthopyroxene and clinopyroxene (Olarewaju, 1987). Olarewaju (1987) proposed a magmatic origin for the coarse-grained and non-foliated charnockitic rocks.

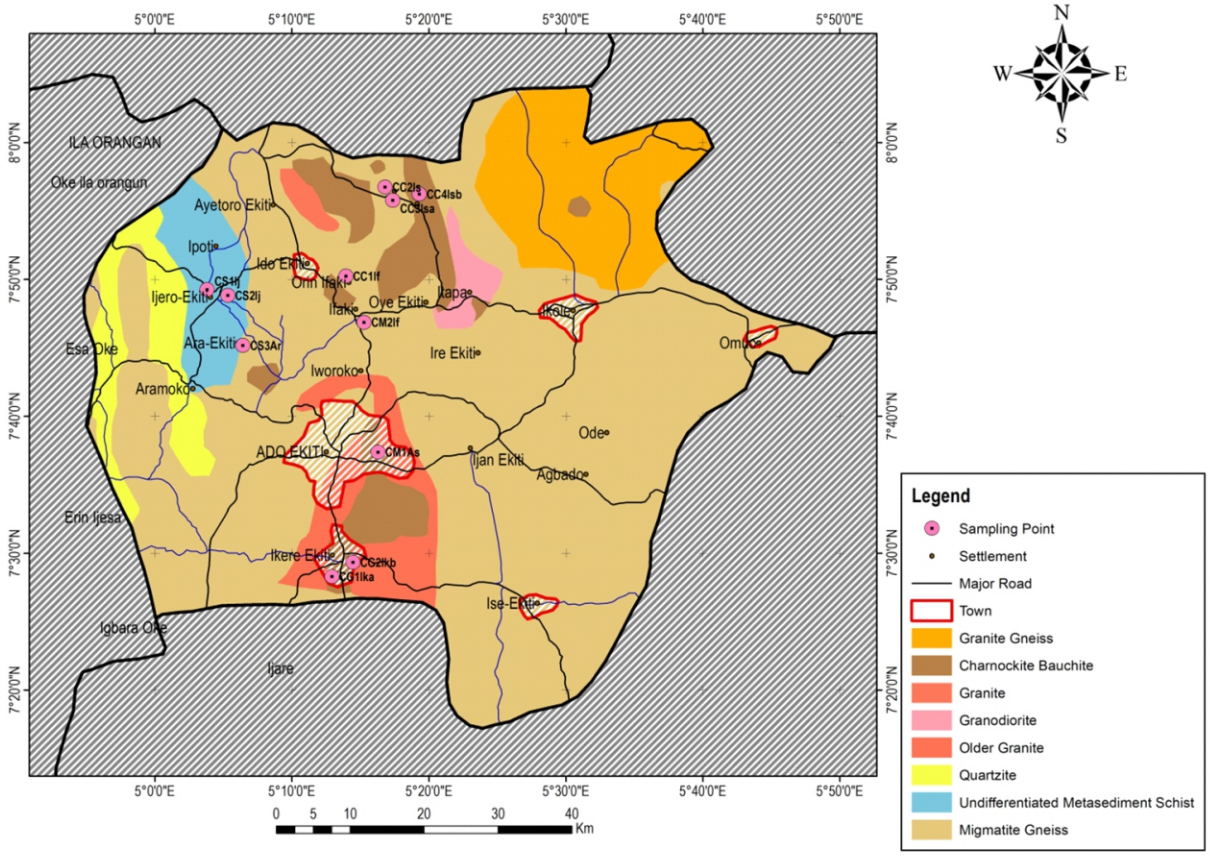

Figure 1: Geology of Ekiti (adapted after Bolarinwa *et al.,* 2017).

METHODS

Sample collection

In order to study the clay occurrences, samples were obtained from Isan, Ijero, Ara and Ikere (the notable clay occurrences) in Ekiti. A total of eleven (11) samples from six clay occurrences over migmatitic gneiss, granite, schist and charnockite were taken from these areas (Figure 1). Sample collection was adapted after FOREGS geochemical mapping field manual (Salminen, *et al.,* 1998) and dependent on size of exposure. Two samples were collected over the migmatitic gneiss at Ado-Ekiti (CM1As) and Ifaki (CM2If); two samples (CG1Ika and CG2Ikb) were collected from the exposures overlying the granite at Ikere; four samples were collected from the exposure overlying the charnockite, one at Ifaki (CC1If) and three at Isan (CC2Is, CC3Isa, CC4Isb). Three samples were collected from exposures overlying metasedimentary rocks: two at Ijero (CS1Ij, CS2Ij) and one at Ara (CS3Ar). Samples collected were kept in well labelled kraft paper bags.

Sample treatment and analyses

Samples were air-dried for about seven days and later disaggregated using the rubber headed pestle and mortar at the Department of Geology, Afe Babalola University, Ado-Ekiti. The disaggregated samples were pulverized using mortar and pestle before sieving through 75 μm to obtain the fine fractions. The sieved samples were subjected to total digestion using four acids (HCl, HNO_3, HF and H_2SO_4). Leached solutions were analysed for elemental concentration using X-Ray Fluorescence Spectrometry (XRF) at ACME Laboratory, Canada. Loss on ignition was determined from the weight loss after subjecting the samples to heat at 1050 °C for two hours.

RESULTS AND DISCUSSION

Geochemical results and parent rock characterisation

Major oxides and trace elements from X-ray fluorescence (XRF) analysis are presented in weight percentages (wt. %) and parts per million (ppm) respectively. The concentrations and elemental ratio are presented in Table 1. The indices of weathering in Table 2 were calculated as molar proportions.

Major oxide geochemistry

Major oxide concentrations (Table 1) revealed variable silica (SiO_2) values with a standard deviation (S.D) of 4.20 for all clay samples in the study. Sample CS3Ar from the clay overlying the schist in Ara has highest SiO_2 concentration (58.03 wt. %) while sample CC1If from Ifaki underlain by charnockite yielded the least at 41.29 wt. %. Geochemical data showed SiO_2 values below Taylor and McLennan's (1985) average crustal abundance of 65.89 wt. %. Alumina (Al_2O_3) concentrations which ranged from 15.86 – 36.61 wt. % were above average continental crust values (15.17 wt. %) reported by Taylor and McLennan (1985). Sample CC2Is from the Isan clay occurrence, underlain by charnockite, yielded the lowest alumina value (15.86 wt. %) which is close to the average crustal value. Samples from exposures overlying the Schist (CS1Ij, 36.61 wt. % and CS2Ij, 34.27 wt. %) and the granite (CG1Ika, 32.17 wt. % and CG2Ikb, 32.21 wt. %) yielded alumina values about twice the average crustal value for alumina. Alumina and Fe_2O_3 values from clay samples from the study compared well with Al_2O_3 and Fe_2O_3 values from kaolin deposits from Egypt (Baioumy *et al.*, 2012), Cameroon and other deposits in Nigeria (Bukalo *et al.*, 2017) which are derived from igneous, metamorphic and sedimentary rocks but were observed to be much higher than the values observed for the hydrothermal kaolin from Argentina (Grecco *et al.*, 2012). Concentrations of Fe_2O_3 in the clay samples from exposures over charnockite and migmatitic gneiss were higher than those observed in samples overlying schist and granite. High Fe_2O_3 and may be linked with Fe^{2+} oxidation during mica expansion (Scott and Youssef, 1978). Sample CC1If over charnockite at Ifaki yielded the highest Fe_2O_3 (13.05 wt. %) while samples from clay occurrences underlain by schist and granite yielded values below 1.0 wt. % except for sample CS3Ar (6.79 wt. %) from Ara underlain by schist and CG2Ikb (2.19) from Ikere. The low Fe_2O_3 values are comparable to the hydrothermal clay from Argentina (Grecco *et al.*, 2012).

Magnesium oxide (MgO) and CaO values were significantly low for most of the samples, that is, less than 1.0 wt. %. Samples CM1As (from exposures underlain by migmatitic gneiss), CC3Isa and CC4Isb (underlain by charnockite) yielded MgO values above 1.00 wt. %. Only one sample (CC4Isb) underlain by charnockite showed CaO value above 1.00 wt. %. This sample yielded the highest CaO (2.07 wt. %) and MgO (1.64 wt. %) values for the study. Low Na_2O values were observed for all samples except CC4Isb (1.82) and CG1Ika (3.35 wt. %). Other samples recorded Na_2O values below 1.00 wt. %. Values of TiO_2 in the clay over migmatitic gneiss, charnockite and granite were observed to be elevated above average crustal value (0.50 wt. %) reported by McLennan and Taylor (1980) and Taylor and McLennan (1985). TiO_2 concentration like Al and Fe is pH-dependent and its enrichment occurs at pH of 4 and 5 (Fortescue, 2012). Elevated TiO_2 concentrations may suggest acidic condition during kaolinisation.

Table 1: Elemental compositions for the clays in Ekiti (major oxides in wt. % and trace elements in ppm).

Element	C**M**1As	C**M**2If	C**S**1Ij	C**S**2Ij	C**S**3Ar	C**C**1If	C**C**2Is	C**C**3Isa	C**C**4Isb	C**G**1Ika	C**G**2Ikb
SiO_2	53.78	46.37	48.27	48.11	58.03	41.29	54.17	49.28	50.34	51.11	50.76
Al_2O_3	21.53	24.13	36.61	34.27	18.93	28.64	15.86	23.05	19.46	32.17	32.21
Fe_2O_3	8.66	10.90	0.67	0.27	6.79	13.05	12.94	8.91	10.00	0.49	2.19
MgO	1.23	0.25	0.05	0.01	0.67	0.27	0.58	1.37	1.64	0.02	0.02
CaO	0.47	0.23	0.01	0.01	0.43	0.23	0.33	0.75	2.07	0.04	0.03
Na_2O	0.29	0.02	0.04	0.02	0.27	0.01	0.51	0.71	1.82	3.35	0.02
K_2O	1.76	0.23	1.37	0.20	3.44	0.25	2.85	2.34	1.98	1.64	0.04
TiO_2	1.08	4.49	0.03	0.01	1.20	2.17	3.73	1.47	2.47	0.01	2.19
P_2O_5	0.05	0.11	0.03	0.03	0.07	0.09	0.07	0.04	0.18	0.06	0.05
MnO	0.08	0.07	0.02	0.01	0.09	0.06	0.13	0.05	0.10	0.01	0.01
Cr_2O_3	0.02	0.02	0.00	0.00	0.01	0.01	0.01	0.01	0.01	0.00	0.02
LOI	10.70	12.90	12.80	17.00	9.70	13.70	8.30	11.60	9.60	11.10	12.30
Sum	99.65	99.72	99.90	99.93	99.63	99.77	99.48	99.58	99.67	99.99	99.84
Ba	560.00	111.00	183.00	107.00	1085.00	94.00	734.00	510.00	435.00	51.00	104.00
Ni	52.00	64.00	21.00	71.00	26.00	82.00	29.00	25.00	23.00	10.00	10.00
Sc	19.00	24.00	1.00	0.05	12.00	23.00	15.00	17.00	20.00	0.05	36.00
Co	22.70	20.00	3.90	11.30	19.70	19.90	28.70	14.40	20.50	3.90	1.60
Hf	18.90	22.50	1.10	4.80	23.90	11.70	42.90	22.90	14.40	8.60	12.70
Zr	731.40	949.90	17.60	46.30	890.30	464.90	1811.00	971.60	585.20	48.80	462.80
Nb	17.80	53.30	217.00	179.60	32.80	37.50	72.30	40.40	60.20	96.20	33.80
Rb	132.00	28.00	282.00	25.00	211.00	30.00	141.00	234.00	177.00	628.00	3.00
Sn	2.00	5.00	38.00	5.00	5.00	4.00	4.00	3.00	4.00	42.00	14.00
Sr	68.40	37.50	8.10	3.90	133.70	32.40	141.60	109.70	288.60	9.30	23.80
Ta	1.10	3.00	39.70	124.10	2.70	2.50	5.80	3.10	5.40	130.80	2.90
Th	33.90	27.70	1.30	0.70	43.90	20.20	41.00	75.90	22.40	8.30	16.80
U	5.30	5.60	3.60	9.00	8.70	4.10	13.30	11.60	9.60	8.80	13.30
V	137.00	229.00	4.00	4.00	105.00	230.00	149.00	84.00	106.00	4.00	261.00
La	97.70	65.90	2.20	2.40	100.60	82.50	95.80	146.20	108.20	0.50	79.60
Ce	185.90	192.20	3.50	4.20	192.50	170.70	235.80	256.50	194.60	0.50	119.60
Pr	19.78	13.87	0.40	0.49	19.06	18.16	19.23	30.88	24.29	0.06	7.92
Nd	71.50	50.60	1.30	2.00	64.20	69.40	66.30	108.60	92.30	0.50	21.00
Sm	11.40	9.36	0.49	0.61	9.83	12.25	11.51	17.84	17.02	0.33	2.96
Eu	1.66	1.99	0.05	0.06	1.75	2.81	2.41	1.68	3.07	0.14	0.49
Gd	9.01	8.11	1.00	0.93	8.38	11.10	9.94	15.07	14.93	1.08	2.57
Tb	1.17	1.23	0.32	0.24	1.16	1.56	1.40	2.02	2.15	0.17	0.35
Dy	6.82	7.25	2.91	1.91	6.49	9.02	7.99	11.14	11.53	1.19	1.87
Ho	1.28	1.46	0.85	0.46	1.31	1.73	1.62	2.27	2.21	0.27	0.34
Er	3.76	4.25	3.10	1.49	3.89	5.00	4.81	6.58	5.84	0.71	0.97
Tm	0.54	0.64	0.47	0.22	0.59	0.68	0.75	0.94	0.84	0.09	0.13
Yb	3.60	4.10	3.14	1.40	3.95	4.15	5.16	5.74	4.88	0.63	0.92
Lu	0.55	0.65	0.47	0.22	0.61	0.66	0.78	0.88	0.72	0.10	0.15
Fe/Mg	8.19	50.80	15.67	19.00	11.86	57.06	25.86	7.51	7.06	34.00	153.00
Ni/Co	2.00	3.00	5.00	6.00	1.00	4.00	1.00	2.00	1.00	3.00	6.00
Nb/Ta	16.00	18.00	5.00	1.00	12.00	15.00	12.00	13.00	11.00	1.00	12.00
Zr/Hf	38.70	42.22	16.00	9.65	37.25	39.74	42.21	42.43	40.64	5.67	36.44
Th/U	6.40	4.95	0.36	0.08	5.05	4.93	3.08	6.54	2.33	0.94	1.26
Rb/Sr	1.93	0.73	34.75	6.51	1.58	0.94	0.99	2.14	0.61	67.53	0.11
Nb/Sr	0.26	1.42	26.79	46.05	0.25	1.16	0.51	0.37	0.21	10.34	1.42

Element	C**M**1As	C**M**2If	C**S**1Ij	C**S**2Ij	C**S**3Ar	C**C**1If	C**C**2Is	C**C**3Isa	C**C**4Isb	C**G**1Ika	C**G**2Ikb
Ba/Sr	8.19	2.96	22.59	27.44	8.12	2.90	5.18	4.65	1.51	5.48	4.37
Ba/Rb	4.24	4.04	0.65	4.21	5.13	3.09	5.22	2.18	2.46	0.08	41.60
La/Yb	27.14	16.07	0.70	1.71	25.47	19.88	18.57	25.47	22.17	0.79	86.52
Sm/Yb	3.17	2.28	0.16	0.44	2.49	2.95	2.23	3.11	3.49	0.52	3.22
La/Lu	177.64	101.38	4.68	10.91	164.92	125.00	122.82	166.14	150.28	5.00	530.67
LREEtot	396.95	342.03	8.94	10.69	396.32	366.92	440.99	576.77	454.41	3.11	234.14
HREEtot	17.72	19.58	11.26	5.94	18.00	22.80	22.51	29.57	28.17	3.16	4.73
LREE/HREEtot	22.40	17.47	0.79	1.80	22.02	16.09	19.59	19.51	16.13	0.98	49.50
Y/Sr	0.53	1.04	4.88	4.59	0.30	1.44	0.33	0.57	0.21	0.98	0.36
Tb/Yb	0.33	0.30	0.10	0.17	0.29	0.38	0.27	0.35	0.44	0.27	0.38
La/Yb(N)	18.30	10.84	0.47	1.16	17.17	13.40	12.52	17.17	14.95	0.54	58.33
La/Sm(N)	5.39	4.43	2.82	2.47	6.44	4.24	5.24	5.15	4.00	0.95	16.92
Tb/Yb(N)	1.43	1.32	0.45	0.76	1.29	1.66	1.20	1.55	1.94	1.19	1.68
Eu/Eu*(N)	0.48	0.68	0.21	0.24	0.58	0.72	0.67	0.31	0.58	0.65	0.53

CM1As – sample from Ado-Ekiti underlain by migmatitic gneiss, CM2If – sample from Ifaki underlain by migmatitic gneiss, CS1Ij and CS2Ij– samples from Ijero underlain by schist, CSAs – sample from Ara underlain by schist, CC1If – sample from Ifaki underlain by charnockite, CC2Is, CC3Isa and CC4Isb – samples from Isan underlain by charnockite, CG1IKa and CG2Ikb – samples from Ikere underlain by granite.

TiO_2 concentration, < 0.5 wt. %, was observed for CS1Ij and CS2Ij. TiO_2 values of 3.73 wt. % and 4.49 wt. % observed for CC2Is (over charnockite) and CM2If (over migmatitic gneiss), respectively, were the highest. Low Fe_2O_3, MgO and TiO_2 compared well with pure kaolin and conformed to the characteristics of porcelain clay (Ojo *et al.*, 2014). Clay samples from areas underlain by schist and granite clustered in plots of SiO_2 vs Al_2O_3 and Fe_2O_3 but behaved relatively univariant in the plot of SiO_2 vs K_2O where SiO_2 values was observed fixed at 40 wt. % for the clays over schist and 50.5 wt. % for the clays over granite respectively while K_2O values varied (Figure 2). A negative correlation was observed for samples of clay overlying the charnockite and the migmatitic gneiss in plots of Fe_2O_3 and Al_2O_3 vs SiO_2.

Sodium oxide and K_2O values were particularly low. Na_2O values were lower than 1.00 wt. % for all samples except for CC4Isb (1.82 wt. %) (over charnockite) and CG1Ika (3.35 wt. %) (over granite). Potash values ranged from 0.04 wt. % (CG2Ikb) to 3.44 wt. % (CS3Ar). The variability in concentration for the alkalis did not suggest control by the underlying rocks and may probably be linked with weathering effects. Ratio of Fe/Mg did not discriminate the clays from different source areas.

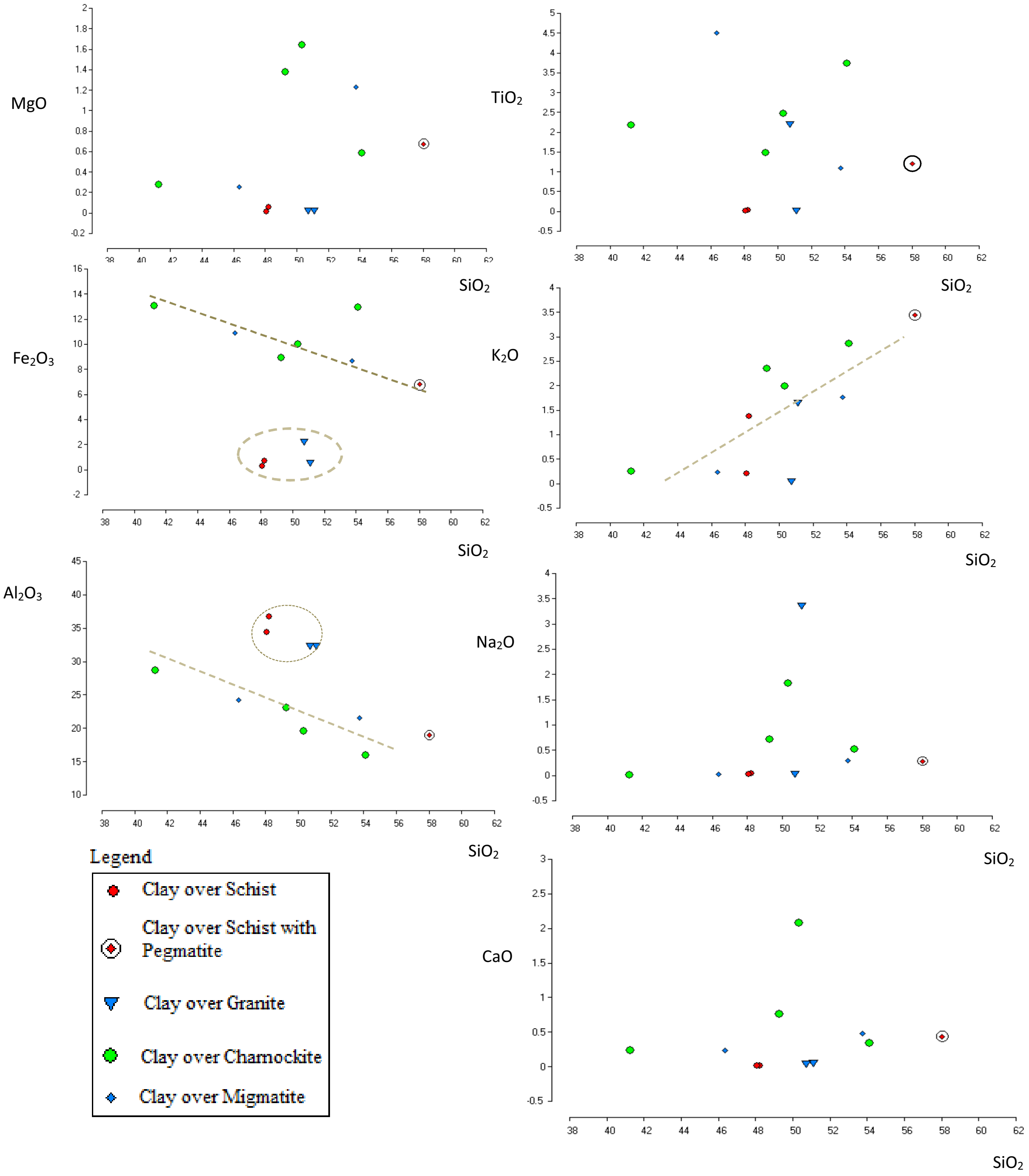

Figure 2: Bivariate plot of SiO$_2$ vs major oxides.

Trace elements

Trace element concentrations for the clay of the study showed variable abundance. Samples CG1Ikb and CS3Ar yielded 51 ppm and 1085 ppm representing the lowest and the highest Ba values respectively. Field observations revealed that the schist in Ara from where this sample (CS3Ar), with the highest Ba, was collected was intruded by pegmatites. The influence of pegmatitic intrusion into the schist at Ara (Okunlola and Jimba, 2006) might have influenced its high concentrations in SiO$_2$, K$_2$O and Ba. Taylor and McLennan (1985) described Rb and Sr among the soluble trace elements. Sr is more enriched in mafic rocks than felsic rocks and therefore more susceptible to weathering than Rb. Variable Rb values, 3 – 628 ppm, were recorded for all samples. Concentrations lower than 10 ppm were observed for Sr in clay samples from the occurrence overlying the schist (CS1Ij, 8.1 ppm and CS2Ij, 3.9

ppm) and one of the samples from occurrence over granite (CG1Ika, 9.3 ppm). Rb, Ba and Cs, examples of large ion lithophile (LIL) elements, are preferentially adsorbed over K_2O on the clay mineral surfaces (Stumm and Morgan, 1981; Middelburg *et al.*, 1988). Trace element ratio of Ba/Sr (Table 1) discriminated the parentage of the clay best when compared with values obtained from other ratios. The Ba/Sr values for samples from Ijero (CS1Ij, 22.51 ppm and CS2Ij, 27.44 ppm), where clay was collected over schist, were higher than that observed for the other samples (Table 1).

Mobility of immobile High Field Strength Elements (HFSE) under processes such as magmatic, metamorphic and hydrothermal alterations has been proposed (Corfu and Davis, 1991; Jiang, 2000; Jiang *et al.*, 2005). In this study, Zr, Hf, and Th yielded high values in clay samples underlain by the migmatitic gneiss, charnockite and granite as well as sample CS3Ar obtained from the occurrence overlying the schist with pegmatitic intrusion. Clay from the occurrences over the schist yielded relatively lower values for these elements (Table 1). Sample CG1Ika also showed low values in Sr, Zr, Hf and Th. The Zr/Hf ratio ranged from 36.44 – 42.21 ppm for samples of clay over the granitoid and the schist with pegmatite. These values were consistent with Taylor and McLennan's (1985) upper continental crust value (33 ppm). Clay samples CS1Ij (16) and CS2Ij (9.65) from the occurrences over the schist and CG1Ika (5.67) over the granite recorded lower values for Zr/Hf ratio (Table 1). Nb and Ta values were higher in the clays from the occurrences over the schistose rocks with the exception of CS3Ar. Values of Nb/Ta ratio for all the samples were consistent with the average upper continent crustal rocks of 12 (Taylor and McLennan, 1985) except CS1Ij (5), CS2Ij (1) and CG1Ika (1) (Table 1). High Th/U, Zr/Hf and Nb/Ta support granitic parentage (Cox *et al.,* 1995).

In the plot of Zr/Hf vs Ba/Sr (Figure 3a), clay with probable granitic parentage were discriminated. Samples CS1Ij, CS2Ij and CG1Ika underlying ferromagnesian mineral rich schist and granite with amphibolite enclaves are discriminated from other clay samples. The clustered samples may reflect parent rocks with enrichment in immobile elements which were not removed during weathering. At high temperatures, Sr behaves relatively immobile. Strontium is used in the Pearce element ratio in figure 3b as the common denominator while Y is used to reflect ferromagnesian mineral rich parentage and Ba to represent the granitic parentage. The plot of Y/Sr vs Ba/Sr (Figure 3b) better discriminated clay from occurrence over the schist from the rest with possible granitic parentage. Low values of Sc, V, Th, and Co for clay occurrences at Ijero (CS1Ij and CS2Ij) and Ikere (CG1Ika) may be indicative of intense weathering they have undergone.

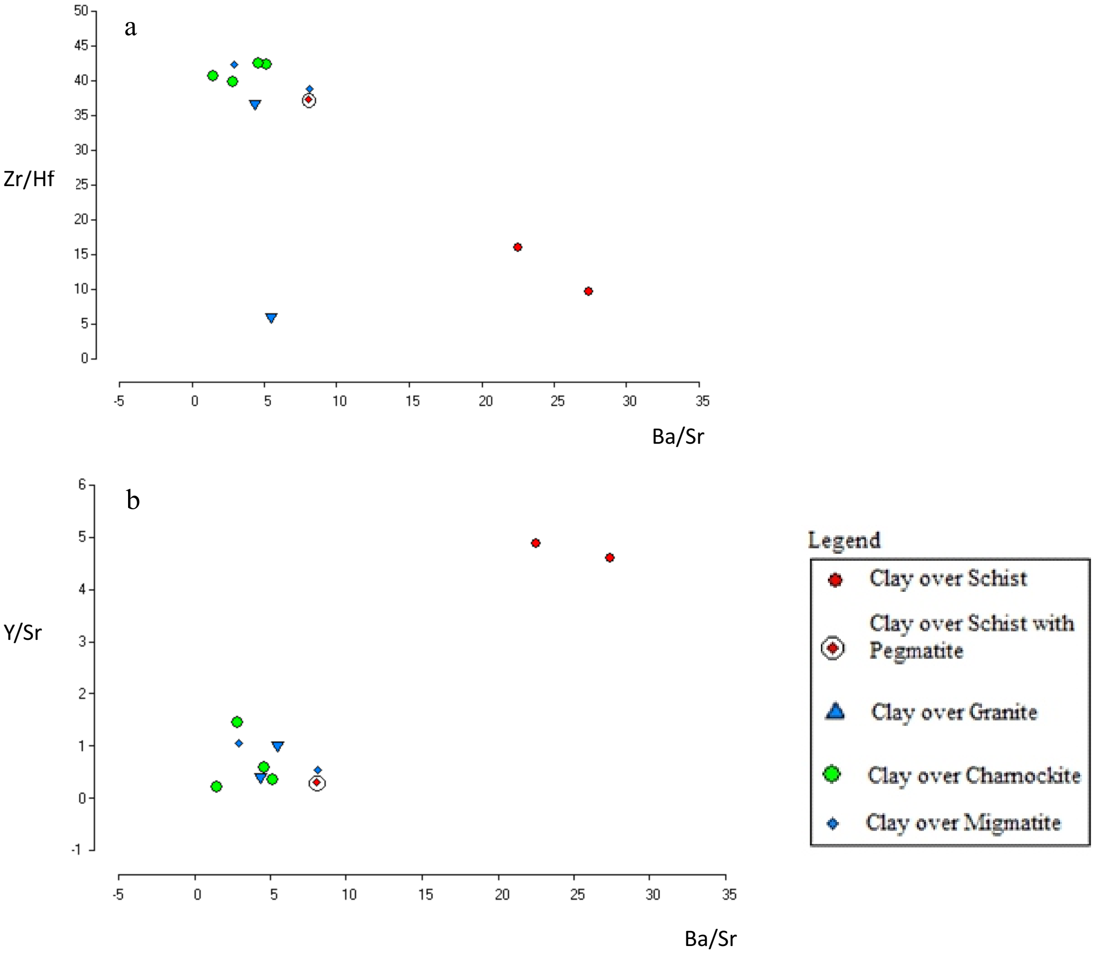

Figure 3: a) Bivariate ratio plot of Zr/Hf vs Ba/Sr. b) Plot of Y/Sr vs Ba/Sr.

Rare earth elements

Rare earth elements are mobilised during weathering and diagenesis but they remain within the weathering profile and therefore are suitable for constraining provenance (Nesbitt, 1979; Sethi *et al.*, 1998, Boggs, 2009). The insoluble nature of REEs in water makes them reliable for provenance studies. The total REE concentrations for the clays revealed values greater than 300 ppm for those overlying charnockite and migmatitic gneiss while lower than 300 ppm were observed for those overlying schistose rocks (CS1Ij, 20.20 and CS2Ij, 16.63) and granite (CG1Ika, 6.27 and CG2Ikb, 238.87).

Lanthanum (La) concentrations for the Ijero clay (CS1Ij, 2.2 ppm and CS2Ij, 2.4 ppm) were lower than that of nearby Ara (CS3Ar, 100.6 ppm) (Table 1). This may be attributed to input from weathering of pegmatites in schists in Ara. Clay samples from other areas yielded higher La values. Clay samples over the charnockite yielded very high La values (82.5 – 146.2 ppm). High total LREE was observed for all samples except for samples CS1Ij, CS2Ij and CG1Ika (Table 1). In order words, high REE(tot) and LREE characterise clays overlying migmatitic gneiss, charnockite and granite which are rocks formed as a result of anatexis and /or magmatism.

REE chondrite normalisation after Boynton (1984) revealed REE enrichment with higher LREE enrichment for clay samples over migmatitic gneiss, charnockite and sample CG2Ikb underlain by granite while samples overlying the Ijero schist (CS1Ij and CS2Ij) and granite (CG1Ika) revealed depleted LREE. REE fractionation in weathered profiles leads to LREE enrichment and HREE depletion (Nesbitt, 1979; Braun *et al.*, 1990). The clays overlying the schist at Ijero (CS1Ij and CS2Ij) and the granite at Ikere (CG1Ika) showed depleted LREE with negative europium anomaly. LREE and HREE depletion was described for the advanced argillic alteration zone in Central Iran (Parsapoor *et al.*, 2009; Grecco *et al.*, 2012).

LREE enrichment with negative europium anomaly agrees with upper continental crust source for the feldspar-rich parent rocks (Figure 4a). Eu anomalies were determined using Eu/Eu* = EuN/(SmN x GdN)1/2, the anomaly values showed weakly negatively europium anomaly (0.21) to moderately high negative europium anomaly (0.72) (Table 1). This may explain a slow to moderately intense dissolution of feldspars in the parent rocks (Mao, *et al.*, 2017). Negative europium anomaly (Eu/Eu*) was observed for all the samples in Figures 4a and b. Residual or meteoric deposits usually display positive Ce anomalies (Ce^{4+}) (Cravero et al., 2001). Cerium normally exists as Ce^{3+} but when oxidised it forms compounds (Cerianite, CeO_2) in the form of Ce^{4+} hence their importance in paleo-redox studies. Positive Ce anomaly was observed for clays over the migmatite (CM2If) and charnockite (CC2Is) (Figure 4a). Figure 4b is a REE plot normalised using North American Shale Composite (NASC) after Haskin and Frey (1966) and revealed flat REE pattern with negative europium anomaly for clay samples overlying migmatitic gneiss, charnockite and sample CG2Ikb over granite. The REE normalisation using UCC values (Figure 4c) showed negative Eu anomaly for clay over the schist (CS1Ij, CS2Ij) and suggests a relatively higher intensity of feldspar dissolution in the clay over the schist.

$La_{(N)}/Yb_{(N)}$ yielded high values for the clay samples except for CS1Ij (0.47), CS2Ij (1.16) and CGIka (0.54). With REEtot of 238.87 ppm, sample CG2Ikb revealed the highest $La_{(N)}/Yb_{(N)}$ (58.33). The plot of $La_{(N)}/Yb_{(N)}$ vs REEtot (Figure 5) revealed samples CS1Ij, CS2Ij and CGIka clustering close to the origin reflecting LREE depletion. Sample CG2Ikb is isolated away from the rest of the samples indicating a high LREE enrichment while the rest of the samples showed a proportionate increase in LREE with total REE. The Nb/Ta vs La plot discriminates samples with upper crustal affinities. Samples in circle show clays with parent rocks having possibly upper crustal affinity (Figure 6). $Tb_{(N)}/Yb_{(N)}$ values for the clays from the schist (CS1Ij and CS2Ij) yielded respective values of 0.45 and 0.76 while other samples had $Tb_{(N)}/Yb_{(N)}$ values greater than 1.0 (Table 1). This suggests relative depletion in HREE in clays from occurrences over the schist. The clays over the schist with least values in the ratio of $Tb_{(N)}/Yb_{(N)}$ have shown relative depletion in both LREE and HREE. Plot of Eu/Eu* vs $Tb_{(N)}/Yb_{(N)}$ discriminates clays formed over schist from granite, charnockite and migmatitic gneiss. Clays from schist are enriched in HREE over clays formed from rocks that crystallized from magmatic fluid or melt (Figure 7).

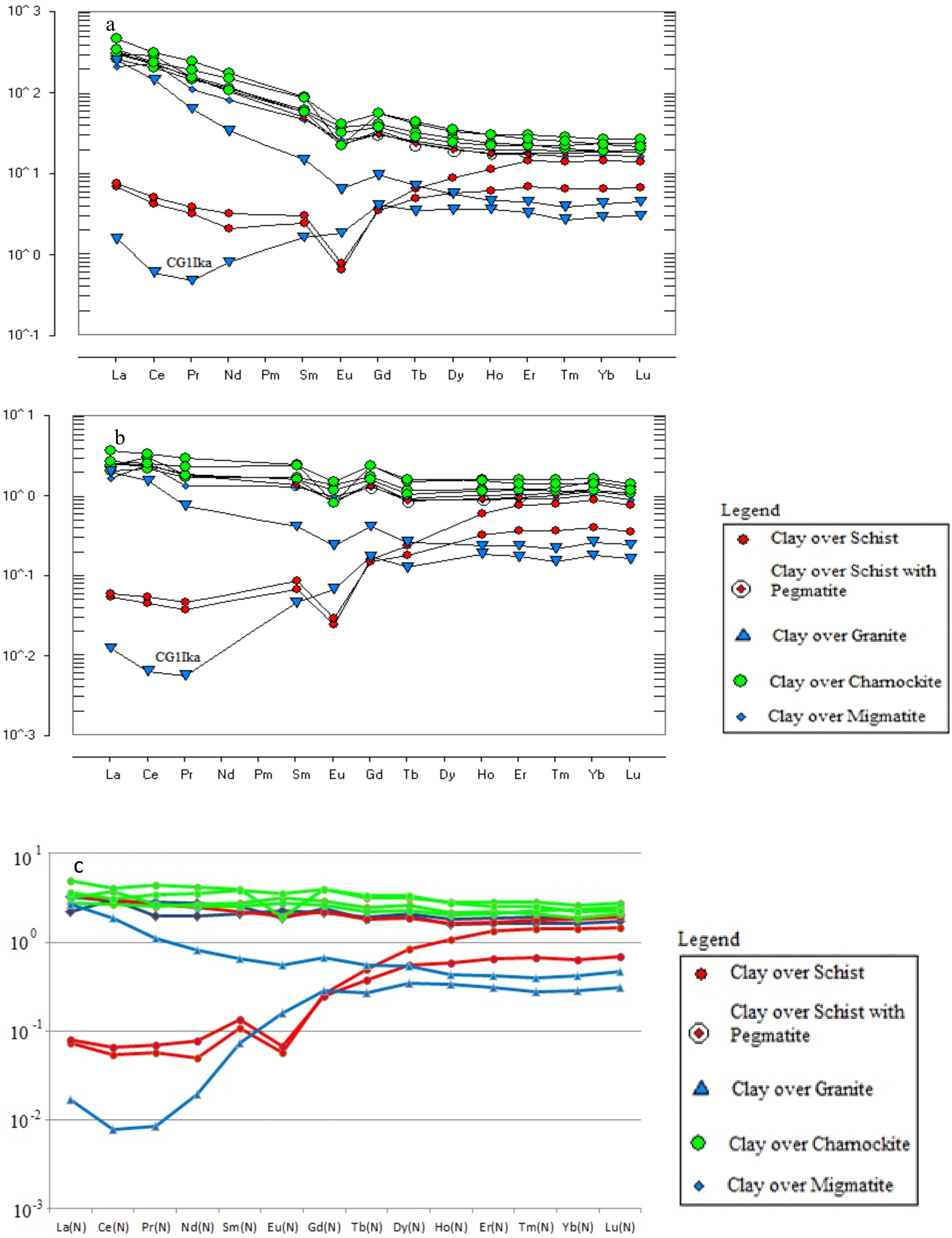

Figure 4: a) Plot of clay samples normalised using chondrite (Boynton, 1984). b) Normalisation using North American Shale Composite (NASC) values after Haskin and Frey (1966). c) Samples normalised using Upper Continental Crust (UCC) values (Taylor and McLennan, 1985).

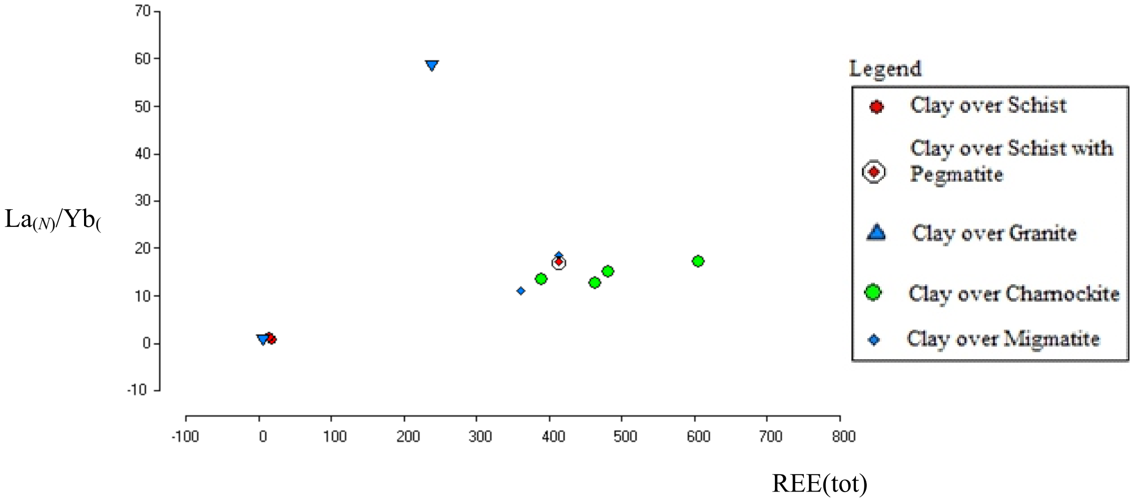

Figure 5: Plot of $La_{(N)}/Yb_{(N)}$ vs REE(tot).

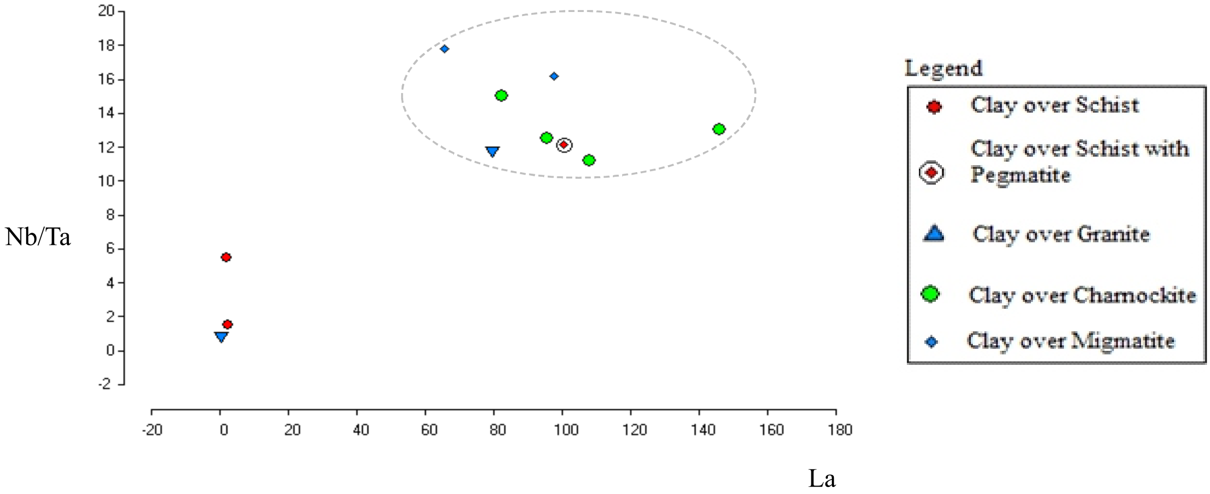

Figure 6: Plot of Nb/Ta vs La.

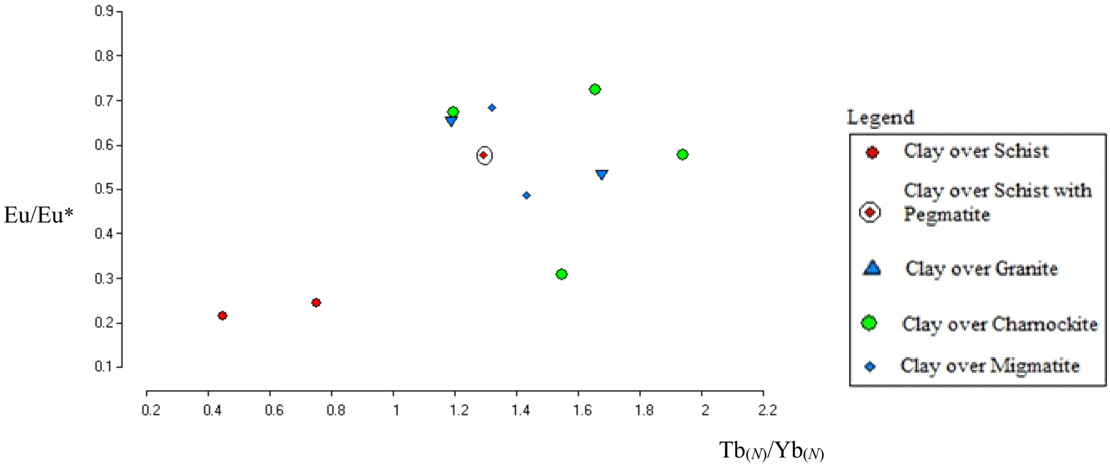

Figure 7: Plot of Eu/Eu* vs $Tb_{(N)}/Yb_{(N)}$.

Paleo-weathering and Precipitation Conditions

The mineral compositions of rocks are broken down when exposed to surficial conditions. The dissolution through processes such as hydrolysis and hydration release ions contained in their crystal lattice in order to become thermodynamically stable (Kasanzu *et al.*, 2008; 2016). A number of researchers have studied the behaviour of major and trace elements during weathering of parent materials and sediments leading to the general agreement that Na, Ca, and Sr are highly mobile while Al, Ti, Fe, Hf, Zr and REEs are relatively immobile (Nesbitt, 1979; Fedo *et al.*, 1995). Elements such as K, Ba, Mg and Rb are also considered immobile because they are easily worn off from primary minerals and adsorbed on the surface of aluminosilicate structures of secondary clay materials in weathering profiles (Kasanzu *et al.*, 2016). However, these elements can also be mobile depending on the degree of weathering. The relative mobility of these elements has been used by Nesbitt and Young, (1984) to determine the extent of weathering by either comparing the ratios of immobile with the mobile elements or by calculating for any of the weathering indices.

Chemical index of alteration (CIA) was calculated in molar proportions and values showed that the clay samples had suffered intermediate to extreme weathering. CIA values calculated using $[Al_2O_3/(Al_2O_3 + CaO^* + K_2O + Na_2O) \times 100]$ $(Where\ CaO^* = CaO - 3.33(P_2O_5))$ revealed moderate to intense weathering for the clays. Fe_2O_3 vs CIA plot (Figure 8a) showed clays underlain by granite and schist as the most weathered occurrences. The plot of Al_2O_3 vs CIA (Figure 8b) revealed a linear relationship indicating progressive weathering from moderate to intense for the clays underlain by charnockite and migmatitic gneiss to those underlain by granite and schist. Index of compositional variability (ICV) was derived using Cox *et al.* (1995) ratio of

$$\frac{CaO+K_2O+Na_2O+Fe_2O_3(t)+MgO+MnO+TiO_2}{Al_2O_3},$$

where $Fe_2O_3(t)$ = total iron and CaO includes all sources of Ca.

ICV values expressed as molecular proportions from their major oxides (wt. %) was calculated to measure the degree of weathering (Cox *et al.*, 1995). Low or decreasing ICV values (that is <1) imply increasing weathering conditions (Cox *et al.*, 1995; Valiani and Rezaee, 2014). The clays revealed ICV values less than 1 (Table 2) for the samples except for clays over the charnockite at Isan (CC2Is, 1.21 and CC4Isb, 1.17). The ICV values agree well with increasing weathering during the formation of clays in the study.

Table 2: Weathering indices (Molecular proportions) obtained for the clay samples of the study.

S/N	CIA	PIA	ICV	MIA[O]	MIA[R]	MgI
CM1As	87	94	0.62	81	65	87
CM2If	98	99	0.59	97	75	97
CS1Ij	96	100	0.06	96	95	100
CS2Ij	99	100	0.01	99	99	100
CS3Ar	80	93	0.67	78	64	92
CC1If	98	99	0.44	97	75	98
CC2Is	78	91	1.21	81	53	92
CC3Isa	82	89	0.70	77	62	87
CC4Isb	70	73	1.17	67	51	82
CG1Ika	82	85	0.24	82	81	100
CG2Ikb	100	100	0.14	100	96	100

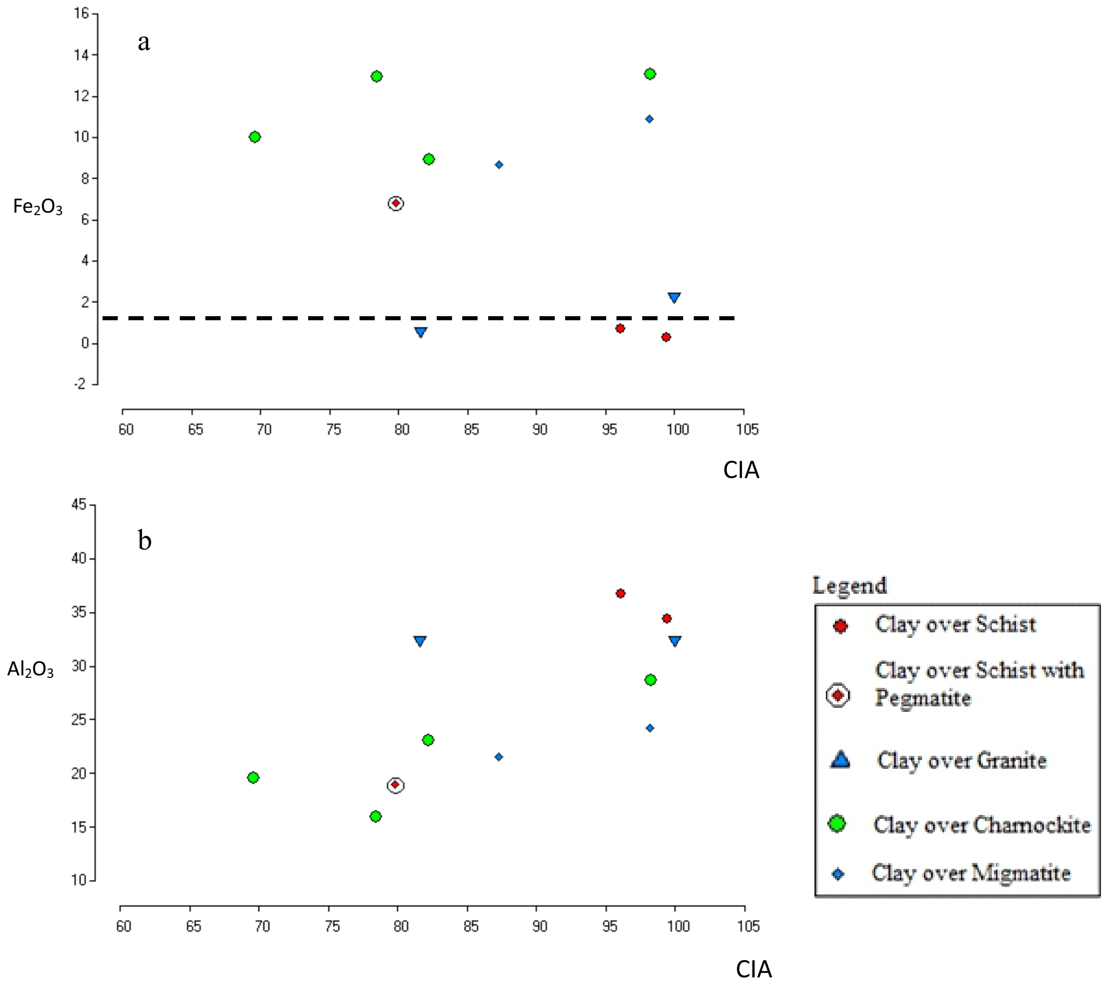

Figure 8: a) Plot of CIA vs Fe_2O_3. b) Linear correlation is observed in the plot of Al_2O_3 vs CIA.

Samples with similar CIA but varying ICV imply different sources (Lee, 2002). The plot of ICV vs CIA (Figure 9) supports varying degrees of weathering for the clays of the study with equally variable parent sources. Clays overlying schist and granite showed intense weathering conditions.

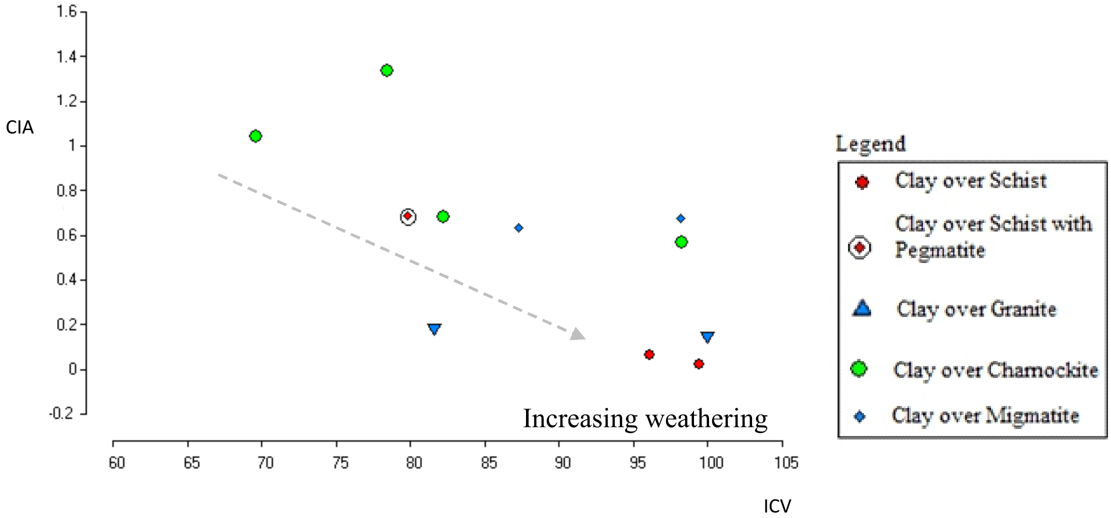

Figure 9: Plot of CIA vs ICV for the clay samples. The clay samples over the schist plotted close to 100 mark of the CIA with low ICV are interpreted as compositionally mature occurrences formed during high degree of weathering.

Plagioclase index of alteration (PIA) (Fedo *et al.*, 1995) uses [($Al_2O_3 – K_2O$)/($Al_2O_3 + CaO + Na_2O - K_2O$) * 100] (in molecular proportions) to monitor plagioclase weathering and values for the studied clays ranged from 73 – 100%. The results showed that the clays overlying charnockite revealed intermediate to intense degrees of weathering. Extreme weathering conditions (hydrolysis) with equally intense removal of ions will alter plagioclase into kaolinite (Nesbitt and Markovics, 1997). PIA values for clays over the schist (CS1Ij, CS2Ij) and granite (CG2Ikb) with 100% and Ni/Co values of 5 and 6 indicate neoformation of possible kaolin occurrences under less oxic conditions. These three samples plotted around the A vertex in the A-CNK-FM plot (Figure 10a). Weathering trend from the plot of A-CNK-FM indicated clays over the schist had suffered intense weathering. Feldspars from the granite and charnockite probably formed illite/kaolinite and smectite in the respective clay occurrences.

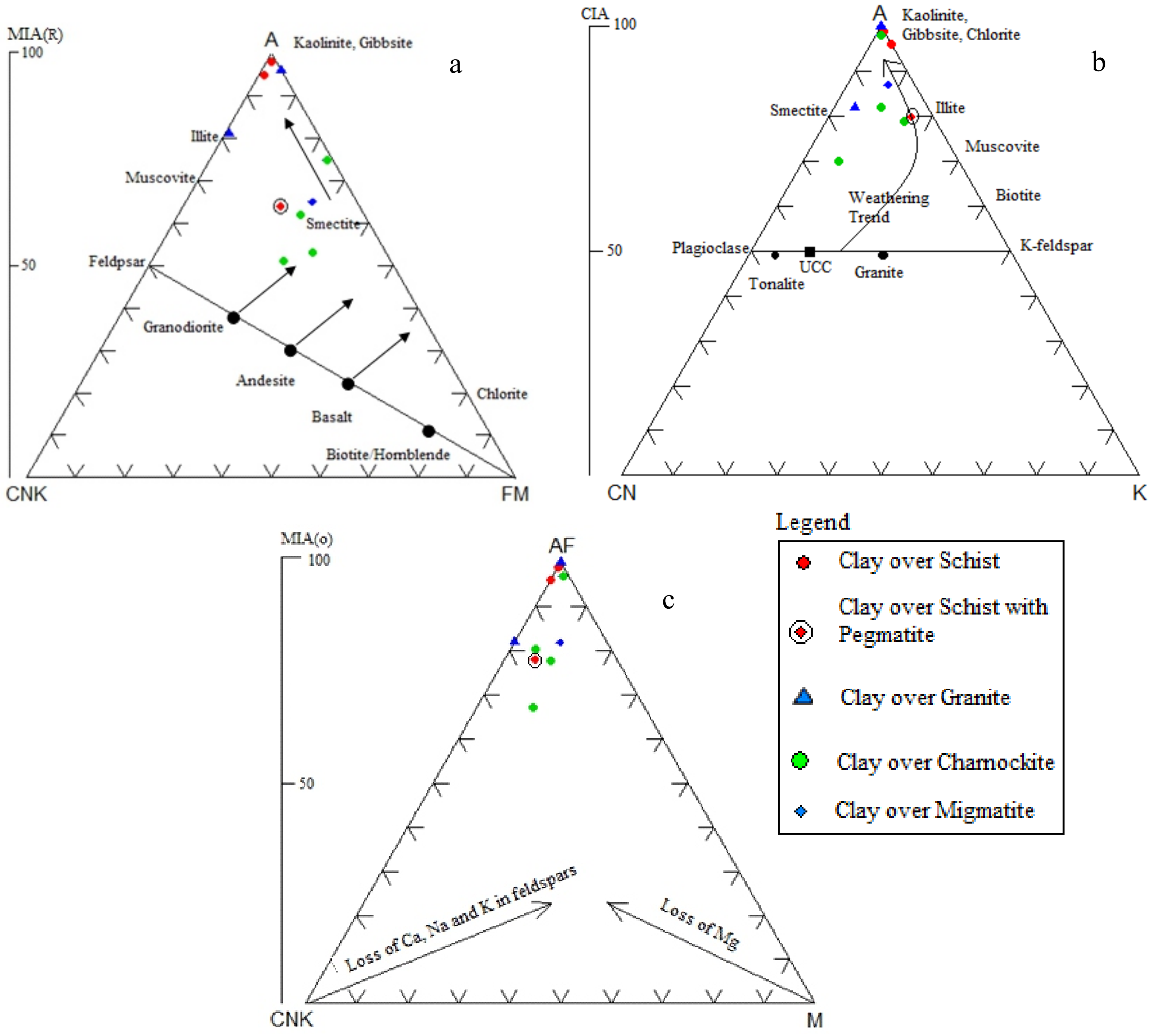

Figure 10: a) The plot of A-CNK-FM (adapted after Nesbitt and Young, 1989) compared with MIA(R) index. b) The CIA index and the plot of A-CN-K (Nesbitt and Young, 1989). c) The AF-CNK-M plot against MIA(O) index (after Babechuk *et al.*, 2014).

Mafic index alteration, expressed in molecular proportions, (MIA) (Babechuk *et al.,* 2014) was developed to evaluate the degradation of ferromagnesian minerals in both oxidative (MIA_O) and reduced (MIA_R) conditions using MIA(O) = 100 x [(Al_2O_3 + Fe_2O_3(T)/(Al_2O_3 + Fe_2O_3(T) + MgO + CaO * + Na_2O + K_2O)] and MIA(R) = 100 x [(Al_2O_3 / Al_2O_3 + Fe_2O_3(T) + MgO + CaO * + Na_2O + K_2O)].

Clays from Ijero (CS1Ij, CS2Ij) and Ikere (CG2Ikb) showed evidence for a less oxic environment and possible leaching of mobile ferrous Fe based on their respective MIA_R values of 95, 99 and 96. Clays from the other occurrences with evidence of oxidised conditions yielded MIA_R values from 51 – 75. Magnesium index (MgI) adapted after Maynard (1992) yielded 100% for clays over Ijero and Ikere. Figures 10 a and b showed that MIA($_{O)}$ and CIA values correlated well in providing evidence of prolonged release of Mg, Ca and Na ions in these clay occurrences.

Provenance and Paleo-redox imprint

The trilinear plot of A-CN-K (after Nesbitt and Young, 1984) suggested plagioclase as the dominant feldspar that weathered to form clay in the study area (Figure 10b). This is consistent with the mineralogy of the dominant rock types in the area (migmatite gneiss and charnockite accounts for 70 – 80% of the total land cover, (Figure 1). The geochemical data did not unequivocally characterise the clays based on their parent rocks. However, the plot of Ba/Sr vs Yb/Sr could serve in discriminating clays with schist as parent rock from other rocks that could have been produced from anatexis and magmatism.

Jones and Manning (1994) proposed Ni/Co, V/Cr and V/V+Ni ratio for evaluating paleo-redox conditions for alteration. They suggested a Ni/Co ratio of <5 to imply oxic conditions, 5 – 7 dysoxic and >7 suboxic to anoxic conditions. Ni/Co ratio of >5 was used as a limit for oxidation in determining paleo-climate conditions. Plots of Ni/Co vs MIA(o) and MIA(R) (Figure 11) showed that clays from Ijero (CS1Ij and CS2Ij) and Ikere (CG1Ika) could have formed under less oxic conditions. Changes in environmental conditions possibly occurred from oxic (Ni/Co <5) to dysoxic (Ni/Co 5 – 7) with increased intensity in weathering. Based on the rock distribution, dysoxic conditions were most likely localised. Clay samples CS1Ij, CS2Ij and CG1Ikb yielded Ni/Co values of 5 and 6 (Table 1) suggestive of a mild reducing condition during weathering and possible mobility of ferrous iron (Fe^{2+}).

Uranium (U) content in clays may be strong indication for a reduced environment (Jones and Manning, 1994). Dypvik and Harris (2001) have used Th/U ratio for such assessment. Th/U values less than 1 were interpreted to indicate U enrichment under reducing conditions. Lesser than 1.0 Th/U values (Table 1) were observed for the Ijero samples (CS1Ij and CS2Ij) suggesting reduced conditions during weathering or association of clay hydrolysate with waters rich in organic content (Milliot, 1970). Th/U values > 1 for Ara (CS3Ij) (schist with pegmatite veins), Isan (Charnockite) and Ikere2 (granite) supports oxidised conditions.

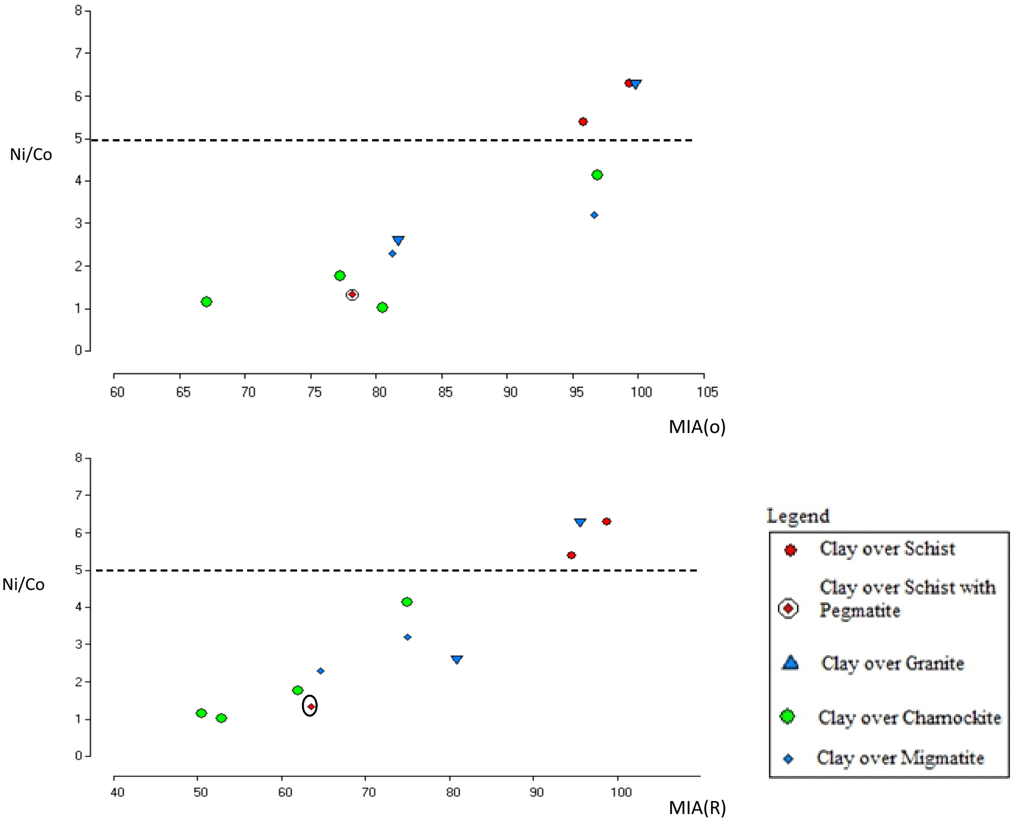

Figure 11: Plots of Ni/Co vs MIA(o) and MIA®.

CONCLUSIONS

In determining parent rock types as sources for the Ekiti clay, major oxide geochemistry (Al_2O_3 and Fe_2O_3) showed concentrations similar to clays derived from igneous and metamorphic rocks but were observed to be much higher in values than that reported for hydrothermally derived kaolin. The plots of Ba/Sr vs Y/Sr and chondrite normalised $(Tb/Yb)_N/(Eu/Eu^*)_N$ discriminated the clays overlying the schist from clays derived, possibly, from rocks that have suffered anatexis or derived from magma. The trilinear plot of AF-CNK-M showed that Ca, Na and K were leached during chemical weathering (kaolinisation). Weathering indices and trilinear plot of A-CNK-FM suggested moderate to intense weathering during the neoformation of the clays in the study. Plagioclase is indicated as the dominant feldspar and that feldspar dissolution under intense weathering affected the REE fractionation. The clays over the schist at Ijero with the lowest ICV values implying increased degree of weathering were depleted in LREE. The plot of Ni/Co vs MIA with Ni/Co of 5 suggested that weathering must have taken place under a dominant oxic condition over localised dysoxic conditions.

ACKNOWLEDGEMENTS

The authors acknowledge the Laboratory assistants at Afe Babalola University for helping in collecting and drying the clay samples and the anonymous reviewers for their constructive criticisms.

REFERENCES

Adelabu, O. S., 2012. Documentation, Application and Utilisation of Clay Minerals in Kaduna State (Nigeria). Clay Minerals in Nature - Their Characterization, Modification and Application. Intech, 3 – 20.

Adeleye, D. R., 1971. Stratigraphy and Sedimentation of the Upper Cretaceous strata around Bida, Nigeria, Ph.D. Thesis University of Ibadan, Nigeria, 297.

Adeleye, D. R. and Dessauvagie, T. F. J., 1972. Stratigraphy of the Niger Embayment near Bida, Nigeria. In Africa Geol. T.F.J. Dessauvagie and A.J. Whiteman (Eds). University of Ibadan Press, (1970), 181 – 186.

Akhirevbulu, O. E., Amadasun, C. V. O., Ogunbajo, M. I. and Ujuanbi, O., 2010. The Geology and Mineralogy of Clay Occurrences Around Kutigi Central Bida Basin, Nigeria. Ethiopian Journal of Environmental Studies and Management, 3, 49 – 56.

Ale, P. T., Dada, J. A. and Adewunmi, A. J., 2014. Industrial Minerals Potentials of Ijero Pegmatite in Ekiti State, Southwestern Nigeria. World Applied Sciences Journal, 29 (3), 415 – 420.

Alege, T. S., Idakwo, S. O., Alege, E. K. and Gideon, Y. B., 2014. Geology, Mineralogy and Geochemistry of Clay Occurrences within the Northern Anambra Basin, Nigeria. British Journal of Applied Science and Technology. 4(5), 841 – 852.

Aramide, F. O., Alaneme, K. K., Olubambi, P. A. and Borode, J. O., 2014. Characterization of some clay deposits in Southwest Nigeria. Leonardo Electronic Journal of Practices and Technology, 25, 46 – 51.

Ayodele, O. S. and Akinyemi, S. A., 2014. Petrostructural and Mineralogical Assessment of the Precambrian Rocks in Ikere Area, Southwestern Nigeria. Asian review of environmental and earth sciences, 1 (3), 66 – 83.

Babechuk, M. G., Widdowson, M. and Kamber, B. S., 2014. Quantifying chemical weathering intensity and trace element release from two contrasting basalt profiles, Deccan Traps, India. Chemical Geology, 363, 56 – 75.

Baioumy, H. M., Gilg, H. A. and Taubald, H., 2012. Mineralogy and geochemistry of the sedimentary kaolin deposits from Sinai, Egypt: Implications for control by the Source rocks. Clays and Clay Minerals, 60 (6), 633 – 654.

Bergaya, F. and Lagaly, G., 2013. General introduction: Clays, Clay minerals and Clay Science. In: F. Bergaya and G. Largaly (eds). Developments in clay science 5, Elsevier Amsterdam, 1 – 19.

Boggs, S., 2009. Petrology of Sedimentary rocks. 2nd Ed. Cambridge University Press The Edinburgh Building, Cambridge CB2 8RU, UK.

Bolarinwa, A., Adeyeri, J. B. and Okeke, T. C., 2017. Compaction and consolidation characteristics of lateritic soil of a Selected site in Ikole Ekiti, Southwest Nigeria. Nigerian Journal of Technology, 36 (21), 339 – 345.

Borst, A. M., Smith, M. P., Finch, A. A., Estrade, G., Villanova-de-Benavent, C., Nason, P., Marquis, E., Horsburgh, N. J., Goodenough, K. M., Xu, C., Kynicky, J. and Geraki, K. 2020. Adsorption of rare earth elements in regolith-hosted clay deposits. Nat. Commun. 11, 4386.

Boynton, W. V., 1984. Geochemistry of the rare earth elements: meteorite studies. In: P. Henderson (ed), Rare Earth Element geochemistry, 63 – 114.

Braun, J. J., Pagel, M., Muller, J. P., Bilong, P., Michard, A., and Guillet, B., 1990. Cerium anomalies in lateritic profiles. Geochimica et Cosmochimica Acta, 54(3), 781 – 795.

Brigatti, M. F., Galan, E. and Theng, B. K. G., 2013. Structure and Mineralogy of Clay minerals. In: F. Bergaya and G. Largaly (eds). Developments in clay science 5, Elsevier Amsterdam, 21 – 81.

Bukalo, N. N., Ekosse, G. E., Odiyo, J. O. and Ogola, J. S., 2017. Geochemistry of selected Kaolins from Cameroon and Nigeria. Open Geosci., 9, 600 – 612.

Corfu, F. and Davis, D. W., 1991. Comment on "Archaean hydrothermal zircon in the Abitibi greenstone belt: constraints on the timing of gold mineralisation", Earth Planet. Sci. Lett., 104, 545 – 552.

Cox, R., Lowe, D. R., & Cullers, R. L., 1995. The influence of sediment recycling and basement composition on evolution of mudrock chemistry in the southwestern United States. Geochimica et Cosmochimica Acta, 59(14), 2919 – 2940.

Cravero M. F., Domı´nguez E. A. and Murray H., 2001. Genesis and applications of the Cerro Rubio kaolin deposit, Patagonia (Argentina). Applied Clay Science, 18, 157 –172.

Dansarai, M. M., Bawa, M. A. and Tokan, A., 2020. Nigerian Clay Deposits for use as Refractory Materials in Metallurgical Industries – A Review, International Journal of Engineering Research & Technology, 9 (6), 707 – 711.

Dypvik, H. and Harris, N. B. 2001. Geochemical facies analysis of fine-grained siliciclastics using Th/U, Zr/Rb and (Zr+ Rb)/Sr ratios. *Chemical Geology,* 181**,** 131 – 146.

Fedo, C. M.; Nesbitt, H. W. and Young, G. M., 1995. Unraveling the effects of potassium metasomatism in sedimentary rocks and paleosols, with implications for paleoweathering conditions and provenance. Geology, 23(10), 921 – 924.

Fortescue, J. A. C., 2012. Environmental Geochemistry: A Holistic Approach. Ecological Studies 35, Springer-Verlag New York, 345.

Galan, E., Aparicio, P., Gonzalez, I., and Miras, A., 1998. Contribution of multivariate analysis to the correlation of some properties of kaolin with its mineralogical and chemical composition. Clay Miner. 33, 65 – 75.

Galan, E. and Ferrell, R. E., 2013. Genesis of clay minerals. In: F. Bergaya and G. Largaly (eds). Developments in clay science 5, Elsevier Amsterdam, 83 – 126.

Grecco, L. E., Marfil, S. A. and Maiza, P. J., 2012. Mineralogy and geochemistry of hydrothermal kaolins from the Adelita mine, Patagonia (Argentina); relation to other mineralization in the area. Clay Minerals, 47, 131 – 146.

Haskin, M. A. and Frey, F. A., 1966. Dispersed and not so rare earth. Sciences, 152, 299 – 314.

Jiang, S.-Y., 2000. Controls on the mobility of high field strength elements (HFSE), U, and Th in an ancient submarine hydrothermal system of the Proterozoic Sullivan Pb-Zn-Ag deposit British Columbia, Canada. Geochemical Journal, 34, 341 – 348.

Jiang, S.-Y; Wang, R.-C; Xu, X.-S. and Zhao, K.-D., 2005. Mobility of high field strength elements in magmatic-, metamorphic- and submarine hydrothermal systems. Elsevier Physics and chemistry of the Earth, 30, 1020 – 1029.

Jones, B. and Manning, D. A. C., 1994. Comparison of geochemical indices used for the interpretation of palaeo-redox conditions in ancient mudstones. Chemical Geology, 111, 111 – 129.

Kasanzu, C. H., Maboko, M. A. H. and Manya, S., 2008. Geochemistry of fine grained clastic sedimentary rocks of the Neoproterozoic Ikorongo group, NE Tanzania: Implications for provenance and parent rock weathering. Precambrian Res. 164, 201 – 213.

Kasanzu, C. H., Maboko, M. A. H. and Manya, S., 2016. Reconstruction of Pliocene-Pleistocene sediment sources and weathering intensity in the paleo-life rich Olduvai and Laetoli basins of northern Tanzania using major and trace element geochemistry and Sr isotopic data. Journal African Earth Sciences 123, 89 – 98.

Lee, Y. I., 2002. Provenance derived from the geochemistry of late Paleozoic–early Mesozoic mudrocks of the Pyeongan Supergroup, Korea. Sedimentary Geology, 149, 219 – 235.

Mao, H., Congqiang, L., Zhiqi, Z. and Junxiong, Y., 2017. Distribution of rare earth elements of granitic regolith under the influence of climate. Acta Geochim 36(3): 440 – 445.

Maynard, J. B., 1992. Chemistry of Modern Soils as a Guide to Interpreting Precambrian Paleosols. Journal of Geology, 100, 279 – 289.

McLennan, S. M. and Taylor, S., 1980. Th and U in sedimentary rocks: crustal evolution and sedimentary recycling. *Nature,* 285**,** 621 – 624.

McLennan, S. M., Hemming, S., McDaniel, D. K. and Hanson, G. N., 1993. Geochemical approaches to sedimentation, provenance, and tectonics. In: M. J., Johnsson, A., Basu, (eds), Processes Controlling the Composition of Clastic Sediments. Geol Soc Am (Special Paper) 284, Boulder, 21 – 40.

Middelburg, J. J., Van der Weijden, C. H. and Woittiez, J. R. W., 1988. Chemical processes affecting the mobility of major, minor and trace elements during weathering of granitic rocks. Chem. Geol., 68, 253 – 273.

Millot, G., 1970. Geology of Clays. Springer-Verlag, New York. 347.

Murray, H. H., 2007. Applied Clay Mineralogy: Occurrences, Processing and Applications of Kaolins, Bentonites, Palygorskite-Sepiolite, and Common Clays. Developments in Clay Science, vol. 2. Elsevier, Amsterdam, 188.

Nesbitt, H. W., 1979. Mobility and fractionation of rare earth elements during weathering of a granodiorite. Nature 279, 206 – 210.

Nesbitt, H. W. and Young G. M., 1984. Prediction of some weathering trends of plutonic and volcanic rocks based on thermodynamic and kinetic considerations. J. Geol. 48, l523 – 1534.

Nesbitt, H. W. and Young, G. M., 1989. Formation and Diagenesis of Weathering Profiles. Journal of Geology, 97, 129 – 147.

Nesbitt, H. W. and Markovics, G., 1997. Weathering of granodioritic crust, long term storage of elements in weathering profiles, and petrogenesis of siliciclastic sediments. Geochimica et Cosmochimica Acta, Elsevier Science., 61 (8), 1653 – 1670.

Obasi, R. A. and Madukwe, H., 2016. Geochemistry, Classification Characteristics Of Pegmatites From Ijero-Ekiti, Ekiti-State, Southwest Nigeria. International Research Journal of Natural Sciences, 4 (4), 1 – 18.

Ojo, O. J., Suraju, A. A. and Alhassan, N., 2014. Geochemical and Mineralogical Studies of Kaolinitic Clays in Parts of Ilorin, Southwestern Basement Rock Area, Nigeria. Universal Jour. of Geosci., 2 (7), 212 – 221.

Okunlola, A. O. and Jimba, S., 2006. Compositional trends in relation to tantalum – niobium mineralisation in Precambrian pegmatites of Aramoko – Ara – Ijero area, southweestern Nigeria. Journal of Mining and Geology, 42, 113 – 126.

Olarewaju, V. O., 1981. Geochemistry of the charnockitic and granitic rocks of the basement complex around Ado Ekiti-Akure, S.W. Nigeria. Ph.D. thesis, Univ. Lond.

Olarewaju, V. O., 1987. Charnockite-granite association in SW Nigeria: rapakivi granite type and charnockitic plutonism in Nigeria? Journal of African Earth Sciences, 6, 67 – 77.

Parsapoor A., Kahlili M. & Mackinzadeh H.A., 2009. The behaviour of trace and rare earth elements (REE) during hydrothermal alteration in the Rangan area (central Iran). Journal of Asian Earth Sciences, 34, 123 – 134.

Rahaman, M. A., 1988. Recent Advances in the Study of the Basement Complex of Nigeria. In Precambrian Geology of Nigeria, Geological Survey of Nigeria, Kaduna South, 11 – 43.

Salminen, R., Tarvainen, T., Demetriades, A., Duris, M., Fordyce, F. M. Gregorauskiene, V., Kahelin, H., Kivisilla, J., Klaver, G., Klein, H., Larson, J. O., Lis, J., Locutura, J., Marsina, K., Mjartanova, H., Mouvet, C., Connor, P. O., Odor, L., Ottonello, G., Paukola, T., Plant, J. A., Reimann, C., Schermann, O., Siewers, U., Steenfelt, A., Van der Sluys, J., de Vivo B. and Williams, L., 1998. FOREGS geochemical mapping. Field manual. Geologian tutkimuskeskus, Opas - *Geological Survey of Finland, Guide* 47, 36 pp.

Scott, A. D. and Youssef, A. F., 1978. Structural iron oxidation during mica expansion. In: M. M. Martland and V. C. Farmer (eds). Proceedings of the VI International Clay Conference, Developments in Sedimentology 27. Elsevier Scientific Publishing Company, 335 Jan van Galenstraat, Netherlands, 17 – 26.

Sethi, P. S., Hannigan, R. E. and Leithold, E. L., 1998. Rare-earth element chemistry of Cenomanian–Turonian shales of the North American Greenhorn Sea, Utah. In: J. Schieber, W. Zimmerle, and P. Sethi (eds.), Shales and Mudstones II: E. Schweizerbart'sche Verlagsbuchhandlung, Stuttgart, 195 – 208.

Stumm, W. and Morgan, J. J., 1981. Aquatic Chemistry. Wiley, New York, 780.

Taylor, S. R. and McLennan, S. M. 1985. The Continental crust: Its Composition and Evolution. Oxford: Blackwell, 312.

Valiani, Z. and Rezaee, P., 2014. Chemical Characteristics, Provenance Determination and Genesis Conditions of Clay Deposits of Kahrizak Formation (Early-Late Pleistocene), East of Tehran, Iran. GSTF International Journal of Geological Sciences, 1 (2), 15 – 22.

Velde, B. and Meunier, A., 2008.The origin of clay minerals in Soils and weathered Rocks. Springer-Verlag Berlin Heidelberg, 426.

Yaraghi, A., Ariffin, K. and Baharun, N. A., 2019. Short Review on REE Recovery from Ion-Adsorption Clays. Aspects Min Miner Sci., 2 (5), 342 – 344.